

# Further evidence for a dynamically generated secondary bow in $^{13}\text{C}+^{12}\text{C}$ rainbow scattering

S. Ohkubo<sup>1</sup>, Y. Hirabayashi<sup>2</sup> and A. A. Ogloblin<sup>3</sup>,

<sup>1</sup>Research Center for Nuclear Physics, Osaka University, Ibaraki, Osaka 567-0047, Japan

<sup>2</sup>Information Initiative Center, Hokkaido University, Sapporo 060-0811, Japan and

<sup>3</sup>RSC “Kurchatov Institute”, RU-123182 Moscow, Russia

(Dated: November 26, 2015)

The existence of a secondary bow is confirmed for  $^{13}\text{C}+^{12}\text{C}$  nuclear rainbow scattering in addition to the  $^{16}\text{O}+^{12}\text{C}$  system. This is found by studying the experimental angular distribution of  $^{13}\text{C}+^{12}\text{C}$  scattering at the incident  $^{13}\text{C}$  energy  $E_L=250$  MeV with an extended double folding (EDF) model that describes all the diagonal and off-diagonal coupling potentials derived from the microscopic wave functions for  $^{12}\text{C}$  using a density-dependent nucleon-nucleon force. The Airy minimum at  $\theta \approx 70^\circ$ , which is not reproduced by a conventional folding potential, is revealed to be a secondary bow generated dynamically by a coupling to the excited state  $2^+$  (4.44 MeV) of  $^{12}\text{C}$ . The essential importance of the quadruple  $Y_2$  term (reorientation term) of potential of the excited state  $2^+$  of  $^{12}\text{C}$  for the emergence of a secondary bow is found. The mechanism of the secondary bow is intuitively explained by showing how the trajectories are refracted dynamically into the classically forbidden angular region beyond the rainbow angle of the primary rainbow.

PACS numbers: 25.70.Bc, 24.10.Eq, 24.10.Ht

Rainbows have been attracting mankind including poets and scientists [1–6] at least two thousand years. A nuclear rainbow in the femto meter world discovered by Goldberg *et al* [7] is a Newton’s zero-order rainbow [8], which was expected by Newton [2] but not realized in meteorological rainbow. The nuclear rainbows have been extensively studied [9] and found to be very important in the studies of nuclear interactions [9–20] and nuclear cluster structures [21–25]. The nuclear rainbows, which carry information about the deep inside of the nucleus, can uniquely determine the interaction potential, that is, the global potential which works over a wide range of energies from negative energy to the high energy region. The existence of a secondary bow is not expected in principle in a nuclear rainbow caused by refraction only. In fact, in the semiclassical theory of nuclear scattering [26–29] in a mean field nuclear potential, only one extremum, (i.e., only one rainbow) is allowed in the deflection function.

Very recently the existence of a secondary bow has been reported [15] in the  $^{16}\text{O}+^{12}\text{C}$  rainbow scattering at around  $E_L=300$  MeV. Its existence has not been noticed in the conventional optical model studies using a folding potential or a phenomenological potential. The secondary bow is generated *dynamically* by a *quantum* coupling effect. Via quantum coupling to an excited state of  $^{12}\text{C}$ , a secondary bow emerges in the classically forbidden dark-side of the ordinary (primary) rainbow caused by a mean field nuclear potential of a Luneburg lens [8]. The dynamical coupling has been shown to cause an additional attraction, which plays a role of a second lens, in the intermediate and inner region of the mean field Luneburg lens potential [18]. It is intriguing and important to explore whether a secondary rainbow, which is logically not limited to the  $^{16}\text{O}+^{12}\text{C}$  system, is confirmed in other systems.

From this viewpoint, when we look carefully at the previously observed experimental data, we notice that the rainbow scattering data for the  $^{13}\text{C}+^{12}\text{C}$  system available at  $E_L(^{13}\text{C})=250$  MeV [30] show an anomaly at large angles in the angular distribution similar to the  $^{16}\text{O}+^{12}\text{C}$  system. It was not possible to describe it in the mean field optical potential model [30].

The purpose of this paper is to report the existence of a secondary bow in  $^{13}\text{C}+^{12}\text{C}$  scattering at  $E_L=250$  MeV. We investigate the angular distribution of  $^{13}\text{C}+^{12}\text{C}$  rainbow scattering using the coupled channels (CC) method with an extended double folding potential and show that a secondary bow is generated dynamically by the coupling to the  $2^+$  (4.44 MeV) state of  $^{12}\text{C}$ . It is revealed that the quadruple  $Y_2$  term (reorientation term) of the potential of the  $2^+$  state is essentially responsible for generating the secondary bow.

We study rainbow scattering for the  $^{13}\text{C}+^{12}\text{C}$  system with an extended double folding (EDF) model that describes all the diagonal and off-diagonal coupling potentials derived from the microscopic realistic wave functions for  $^{12}\text{C}$  using a density-dependent nucleon-nucleon force. The diagonal and coupling potentials for the  $^{13}\text{C}+^{12}\text{C}$  system are calculated using the EDF model as follows,

$$V_{ij}(\mathbf{R}) = \int \rho_{00}^{(^{13}\text{C})}(\mathbf{r}_1) \rho_{ij}^{(^{12}\text{C})}(\mathbf{r}_2) \times v_{NN}(E, \rho, \mathbf{r}_1 + \mathbf{R} - \mathbf{r}_2) d\mathbf{r}_1 d\mathbf{r}_2, \quad (1)$$

where  $\rho_{00}^{(^{13}\text{C})}(\mathbf{r})$  is the diagonal nucleon density of the ground state of  $^{13}\text{C}$  taken from Ref. [31].  $\rho_{ij}^{(^{12}\text{C})}(\mathbf{r})$  represents the diagonal ( $i=j$ ) or transition ( $i \neq j$ ) nucleon density of  $^{12}\text{C}$  which is calculated using the microscopic three  $\alpha$  cluster model in the resonating group method [32]. This model reproduces the  $\alpha$  cluster and shell-like structures of  $^{12}\text{C}$  well and the wave functions have been

checked for many experimental data including charge form factors, electric transition probabilities [32] and the quadrupole moment of the  $2^+$  (4.44 MeV) state [33]. We take into account the excitation of the  $2^+$  and  $3^-$  (9.64 MeV) states of  $^{12}\text{C}$  in the calculations. For the effective interaction  $v_{\text{NN}}$  we use the DDM3Y-FR interaction [34], which takes into account the finite-range nucleon exchange effect [35]. We introduce the normalization factor  $N_R$  [36–38] for the real double folding potential. An imaginary potential with a Woods-Saxon volume-type (nondeformed) form factor is introduced phenomenologically to take into account the effect of absorption due to other channels. It has been shown in many coupled channel studies of rainbow scattering involving  $^{12}\text{C}$  [12–16] that effects of densely populated high-lying excited states, including the energy region of giant resonances, can be well expressed by an imaginary potential. A complex coupling, which is often used but has no rigorous theoretical justification especially when the projectile is composite [39], is not introduced because without it the present EDF model successfully reproduced many rainbow scattering data systematically over a wide range of incident energies [12–19, 25].

The nuclear rainbow in  $^{13}\text{C}+^{12}\text{C}$  scattering was first observed by Bohlen *et al.* [40] at  $E_L=260$  MeV. The experimental angular distributions measured up to  $\theta=60^\circ$  were reproduced in the optical model and CC calculations with a phenomenological Woods-Saxon potential. Recently the measurement was extended at  $E_L=250$  MeV to larger angles up to  $\theta=94^\circ$  in Ref. [30]. We note that it was impossible to reproduce the experimental angular distribution, which does not fall off monotonically beyond  $\theta\approx 70^\circ$ , in the optical model calculations with a phenomenological Woods-Saxon potential [30]. This discrepancy between the calculation and the experimental data at large angles in rainbow scattering is reminiscent of the similar difficult situation encountered in  $^{16}\text{O}+^{12}\text{C}$  scattering at around  $E_L=300$  MeV [11], which was solved by noticing the existence of a secondary bow generated dynamically [15].

In Fig. 1(a) the angular distributions in elastic  $^{13}\text{C}+^{12}\text{C}$  scattering calculated at  $E_L=250$  MeV using the single channel double folding (DF) potential without channel couplings (dotted line) and CC with EDF are displayed in comparison with the experimental data. We take  $N_R=1.2$  for the real potential. For the imaginary potential the strength parameter  $W=20$  MeV was found to fit the data while the radius parameter and the diffuseness parameter were fixed at  $R=5.6$  fm and  $a=0.7$  fm, respectively. The same imaginary potential parameters are used both in the single channel and CC calculations throughout this paper. We see that the single channel calculation gives the first Airy minimum  $A1^{(P)}$  at  $\theta=45^\circ$  with the broad Airy maximum  $A1$  at  $\theta=55^\circ$  followed by a falloff of the cross sections in the darkside region. This  $A1^{(P)}$  minimum corresponds well to the observed Airy minimum at  $\theta=45^\circ$  in the experimental data. In the single channel calculation, however, the structure observed

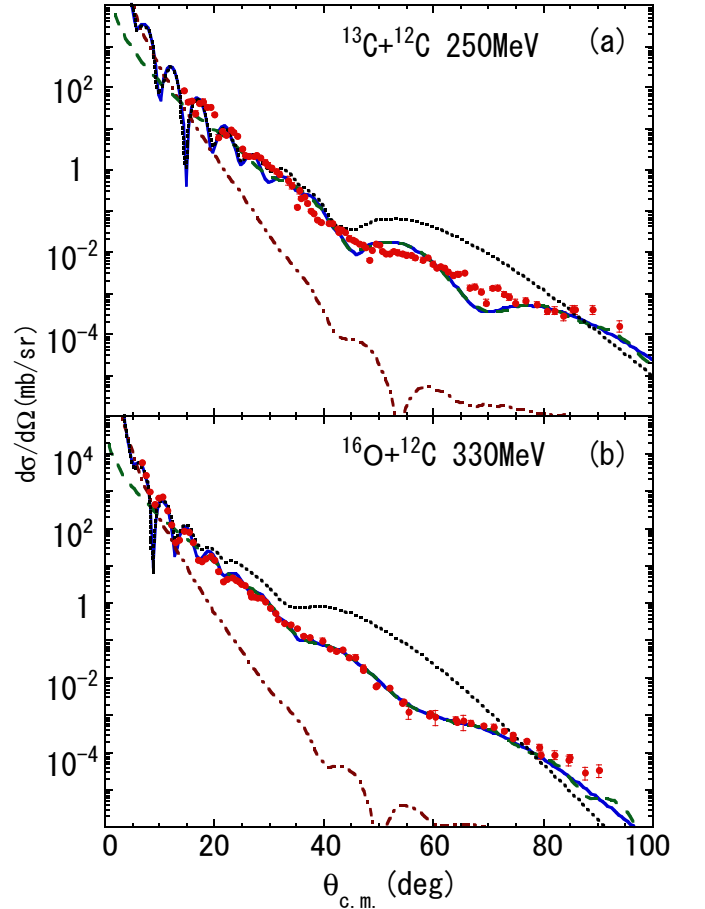


FIG. 1: (Color online) Angular distributions in (a)  $^{13}\text{C}+^{12}\text{C}$  scattering at  $E_L=250$  MeV and (b)  $^{16}\text{O}+^{12}\text{C}$  scattering at  $E_L=330$  MeV obtained using the CC method (blue solid lines) and single channel (dotted lines) calculations are displayed in comparison with the experimental data (points) from Refs.[30, 41]. The farside and nearside components of the CC calculations are shown by the green dashed lines and the brown dash-dotted lines, respectively. The CC results are obtained in panel (a) with coupling to the  $2^+$  and  $3^-$  states of  $^{12}\text{C}$  and in panel (b) with coupling to the  $2^+$  and  $3^-$  states of  $^{12}\text{C}$  and  $^{16}\text{O}$ . The potential parameters used in (b) are taken from Ref.[15].

beyond  $\theta=60^\circ$  is missing.

The CC calculation with coupling to the  $2^+$  and  $3^-$  states of  $^{12}\text{C}$  is displayed by the blue solid line, which does not fall off monotonically beyond  $\theta=60^\circ$  and gives a minimum at  $\theta=70^\circ$  in accordance with the experimental data. The calculated cross sections are decomposed into the farside (green dashed line) and nearside (brown dash-dotted line) components. Beyond  $\theta=30^\circ$  the nearside contribution decreases rapidly and the scattering is dominated by the refractive farside scattering. It is difficult to see the difference between the solid line and dashed line in Fig. 1(a). The minimum at  $\theta=70^\circ$  is caused by refractive farside scattering. Thus it is obvious that this minimum located in the darkside region of the primary

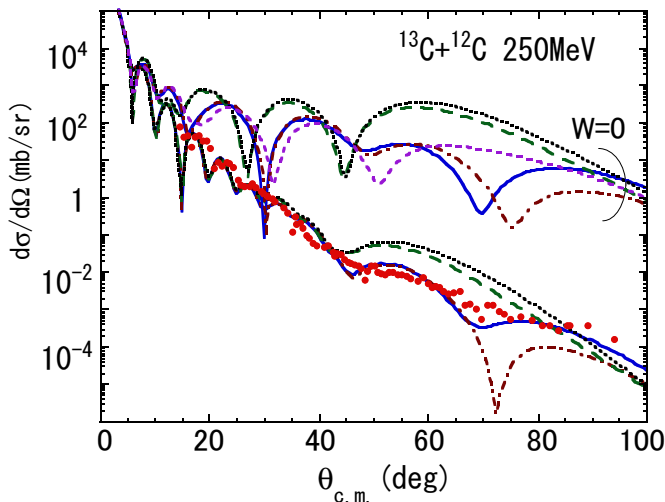


FIG. 2: (Color online) Angular distributions in  $^{13}\text{C}+^{12}\text{C}$  scattering at  $E_L=250$  MeV calculated using the CC method and a single channel (black dotted lines) are displayed in comparison with the experimental data (points) [30]. The blue solid, brown dash-dotted and green long-dashed lines represent the CC results with coupling to both the  $2^+$  and  $3^-$  states of  $^{12}\text{C}$ , those with coupling to the  $2^+$  state only and those with coupling to the  $3^-$  state only, respectively. The upper figures ( $W=0$ ) are calculated by switching off the imaginary potential. The purple short-dashed line represents the CC calculations with coupling to the  $2^+$  state *without* the quadrupole  $Y_2$  term (reorientation term) for  $^{12}\text{C}(2^+)$ .

rainbow is not caused by the primary rainbow due to the Luneburg lens [8] of the static mean field nuclear potential. It is the Airy minimum  $A1^{(S)}$  of the secondary rainbow caused dynamically by the channel coupling to the excited states of  $^{12}\text{C}$ . This is reinforced by comparing it with the secondary bow that appears in  $^{16}\text{O}+^{12}\text{C}$  scattering systematically. In Fig.1(b) the angular distributions in elastic  $^{16}\text{O}+^{12}\text{C}$  scattering at  $E_L=330$  MeV are displayed. In the CC calculations with coupling to the  $2_1^+$  and  $3_1^-$  states of both  $^{12}\text{C}$  and  $^{16}\text{O}$  are included. The behavior of the experimental and calculated angular distributions in  $^{13}\text{C}+^{12}\text{C}$  scattering resembles that of  $^{16}\text{O}+^{12}\text{C}$  scattering where a secondary rainbow appears with the Airy minimum  $A1^{(S)}$  at around  $\theta=60^\circ$  in addition to the Airy minimum  $A1^{(P)}$  of the primary rainbow at  $\theta=40^\circ$  [15]. We note here that the contribution of the elastic transfer (one nucleon exchange) contributions is small in the relevant angular region and does not contribute to the structure of the Airy minimum. In fact, Bohlen *et al.* [40] measured  $^{12}\text{C}(^{13}\text{C}, ^{12}\text{C})^{13}\text{C}$  one nucleon transfer reaction cross sections at  $E_L=260$  MeV, which decrease rapidly toward large angles.

We investigate what coupling is responsible for the generation of the Airy minimum  $A1^{(S)}$  at  $\theta=70^\circ$ . In Fig. 2 the angular distributions calculated with coupling to the  $2^+$  state only and coupling to the  $3^-$  state only are individually displayed. The calculated results with coupling to the  $3^-$  state (green dashed lines) are essentially simi-

lar to those in the single channel calculation (black dotted lines) and do not show the Airy minimum  $A1^{(S)}$  at  $\theta=70^\circ$ . On the other hand, the calculated results with coupling to the  $2^+$  state (brown dash-dotted lines) show a deep Airy minimum at  $\theta=75^\circ$ . By including the coupling to the  $3^-$  state, as shown by the blue solid line, this deep Airy minimum is smeared and shifted forward slightly approaching the experimental Airy minimum. The addition of coupling to the  $3^-$  state plays a role of introducing an imaginary potential. The origin of the Airy minimum is more clearly confirmed in the calculations by switching off the imaginary potentials. The position of the Airy minimum in the calculation with coupling to the  $3^-$  state ( $W=0$  green dashed line) is the same as that in the single channel calculation ( $W=0$  black dotted line). In the calculation with coupling to the  $2^+$  state with  $W=0$  (brown dash-dotted lines), the additional Airy minimum is created at  $\theta=75^\circ$ , which is shifted forward about  $5^\circ$  by including the coupling to the  $3^-$  state (blue solid). It is clear that the Airy minimum at  $\theta=70^\circ$  is generated dynamically by the coupling to the  $2^+$  state of  $^{12}\text{C}$ . The generation mechanism of the Airy minimum is completely different from that at around  $\theta=40^\circ$  due to the static mean field nuclear potential of a Luneburg lens [8]. Thus the Airy minimum  $A1^{(S)}$  at  $\theta=70^\circ$  is the same kind of secondary bow that was found in the  $^{16}\text{O}+^{12}\text{C}$  system in Ref. [15].

We investigate further which part of the quadrupole  $Y_2$  term (reorientation term) and coupling potentials is dominantly important in generating the secondary bow. The diagonal potential for  $^{12}\text{C}(2^+)$  has a  $Y_2$  term (reorientation term) in the multipole expansion. In Fig. 2 the angular distribution calculated using the CC method with coupling to the  $2^+$  state but *without* the quadrupole  $Y_2$  term of the potentials for  $^{12}\text{C}(2^+)$  is displayed for the  $W=0$  case by the purple short-dashed line. The difference between the brown dash-dotted line and the purple short-dashed line in the  $W=0$  case is due to the quadrupole  $Y_2$  term for the  $2^+$  state. As we see in the purple short-dashed line, the Airy minimum at  $\theta=75^\circ$  of the secondary bow disappears if the  $Y_2$  term is not included. Thus it is found that the quadrupole  $Y_2$  term of the potential for  $^{12}\text{C}(2^+)$  causes strong refraction and is essentially responsible for the generation of the Airy minimum of the secondary bow.

How a secondary bow is physically created by the coupling to the  $^{12}\text{C}(2^+)$  was quantitatively investigated for the  $^{16}\text{O}+^{12}\text{C}$  system in Ref.[15]. By using an inversion technique it was found in Ref.[18] that a dynamical attractive potential is induced by the coupling to the collective excited state  $2^+$  state of  $^{12}\text{C}$ . In Fig. 3 refraction of the trajectories in the classical picture in nuclear rainbow scattering is displayed. As shown in Fig. 3(a), when there is no coupling to the excited state, the refracted angle  $\theta_R$  is the largest (deflection) angle (rainbow angle of the primary bow) among all the incident classical trajectories that are refracted in the nuclear optical potential (Luneburg lens). Refraction beyond  $\theta_R$  is classi-

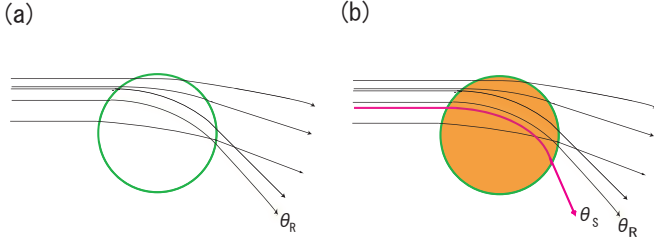


FIG. 3: (Color online) The illustrative figures of refractive trajectories by the attractive potential in nuclear rainbow scattering. (a) Refraction in the case without coupling. The refracted angle  $\theta_R$  is a rainbow angle for the primary nuclear rainbow caused by the optical potential (Luneburg lens) of the nucleus (indicated by a circle). The angular region  $\theta \leq \theta_R$  is the bright side of the primary nuclear rainbow.  $\theta > \theta_R$  is not allowed to refract classically and is the darkside. (b) Refraction in the case with coupling to the collective excited  $2^+$  state of  $^{12}\text{C}$ . The trajectories of a secondary bow (red line) strongly refracted (refracted angle  $\theta_S$ ) beyond  $\theta_R$  by the additional attractive potential in the inner region induced dynamically by the coupling to the excited state of the nucleus.

cally forbidden. Therefore the angular region larger than  $\theta_R$  becomes completely dark in classical mechanics. In quantum mechanics cross sections falls rapidly beyond  $\theta_R$  in the angular distribution as seen in the dotted line in Fig. 1(a). However, as shown in Fig. 3(b), when there is quantum coupling to the  $2^+$  state of  $^{12}\text{C}$  state, classically forbidden refraction beyond  $\theta_R$  becomes possible and can be enhanced. This is because the coupling to the collective excited state plays a role of a second lens, as discussed in Ref.[15], creating a characteristic polarization potential, especially attractive by nature in the internal region [18]. As shown by the red line in Fig. 3(b), trajectories can be refracted to larger angles beyond  $\theta_R$  by the induced attraction in addition to the Luneburg lens potential. Thus the refraction beyond  $\theta_R$  is enhanced and the largest refractive angle, i.e., a second deflection angle  $\theta_S$  appears in the dark side of the primary nuclear rainbow. This is the secondary bow created on the darkside,  $\theta > \theta_R$ , of the conventional primary nuclear rainbow as seen in the solid line in Fig. 1(a).

Although there are no angular distribution data available up to the large angles around  $\theta=90^\circ$  in  $^{13}\text{C}+^{12}\text{C}$  elastic scattering except  $E_L=250$  MeV, it is theoretically expected that a secondary rainbow appears at other energies. In Fig. 4 the angular distributions calculated using the CC method with coupling to the  $2^+$  and  $3^-$  states are displayed in comparison with the single channel calculations for  $E_L=200, 260$  and  $330$  MeV. In all the calculations  $N_R=1.2$  for the real potentials and the same potential parameters are used for the imaginary potentials. The real potential has energy dependence through that of the two-body effective interaction DDM3Y-FR [34]. The volume integral per nucleon pair of the real potential,  $J_V$ , is 331, 316, 314, and 296 MeVfm<sup>3</sup> for  $E_L=200, 250, 260$  and  $330$  MeV, respectively. The calculations show the

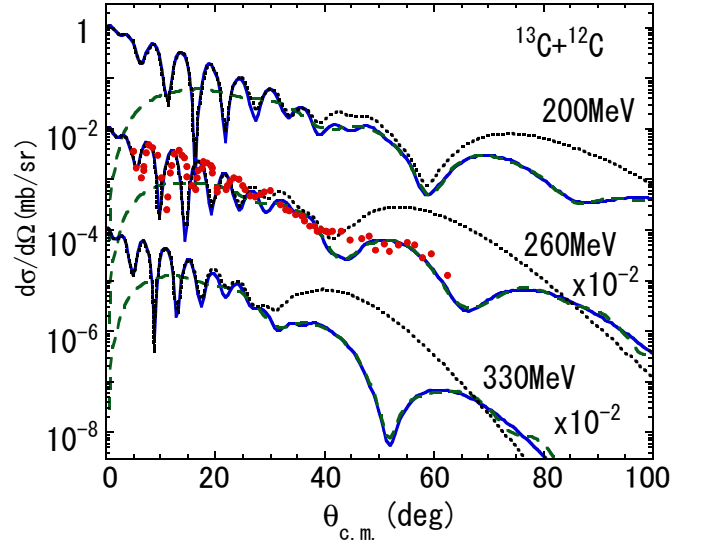


FIG. 4: (Color online) The energy evolution of the Airy structure in the angular distributions of the cross sections in  $^{13}\text{C}+^{12}\text{C}$  scattering calculated with coupling to the  $2^+$  and  $3^-$  states of  $^{12}\text{C}$  (blue solid lines) and the farside components (green dashed lines) are displayed at  $E_L=200, 260$  and  $330$  MeV in comparison with the experimental data (points) from Ref.[40]. The dotted lines represent the single channel calculation.

emergence of the Airy minimum  $A1^{(S)}$  of the secondary bow at  $\theta \approx 90^\circ$  for  $E_L=200$  MeV and at  $\theta \approx 65^\circ$  for  $E_L=260$  MeV. At the higher energy of  $E_L=330$  MeV a sharper Airy minimum of the secondary bow is created dynamically by the channel coupling. These Airy minima are essentially created by the coupling to the  $2^+$  state of  $^{12}\text{C}$ . As the incident energy increases, the Airy minimum  $A1^{(S)}$  shifts to forward angles. It is highly desired to measure the energy evolution of the Airy minimum in the angular distributions in  $^{13}\text{C}+^{12}\text{C}$  elastic scattering.

To summarize, we have shown the evidence for the existence of a secondary rainbow in the angular distribution in  $^{13}\text{C}+^{12}\text{C}$  scattering at  $E_L=250$  MeV. This was achieved by analyzing the experimental angular distribution using a coupled channel method with an extended double folding (EDF) potential derived from the microscopic wave functions for  $^{12}\text{C}$ . The minimum at  $\theta \approx 70^\circ$  in the experimental angular distribution, which is not reproduced by the conventional optical potential model, is reproduced by the coupled channel calculations and found to be an Airy minimum of the secondary bow. It is found that the secondary nuclear rainbow is caused by coupling to the  $2^+$  state of  $^{12}\text{C}$  and the quadrupole  $Y_2$  term (reorientation term) of the potential for the  $2^+$  state is essentially responsible for the creation of the secondary bow. The mechanism of the generation of the secondary bow is intuitively explained by showing how the trajectories are refracted dynamically into the classically forbidden angular region beyond the rainbow angle of the primary rainbow.

One of the authors (SO) thanks the Yukawa Institute for Theoretical Physics, Kyoto University for the hospitality extended during a stay in May 2015. A. O.

was partly supported by Russian Scientific Foundation (Grant No. RNF14-12-00079).

- 
- [1] R. Descartes, *Le Discours de la methode* (sous-titre Pour bien conduire sa raison, et chercher la verité dans les sciences) plus la Dioptrique, Les Meteores et la Geometrie (Leiden, 1637; Hackett Publishing, Cambridge, 2001).
  - [2] I. Newton, *Opticks or, a Treatise of the Reflexions, Refractions, Inflexions and Colours of Light* (London, 1704); (Dover publications, New York, 1952).
  - [3] H. M. Nussenzveig, *Sci. Am.* **236**, 116 (1977).
  - [4] R. Greenler, *Rainbows, Halos and Glories* (Cambridge University Press, Cambridge, 1980).
  - [5] J. A. Adam, *Phys. Rep.* **356**, 229 (2002).
  - [6] B. Matte, *Historie de l'arc-en-ciel* (Édition du Seuil, Paris, 2005); M. Blay, *Les figures de l'arc-en-ciel* (Belin, Paris, 2005).
  - [7] D. A. Goldberg, S. M. Smith, and G. F. Burdzyk, *Phys. Rev. C* **10**, 1362 (1974).
  - [8] F. Michel, G. Reidemeister, and S. Ohkubo, *Phys. Rev. Lett.* **89**, 152701 (2002).
  - [9] D. T. Khoa, W. von Oertzen, H. G. Bohlen, and S. Ohkubo, *J. Phys. G* **34**, R111 (2007) and references therein.
  - [10] D. T. Khoa, W. von Oertzen, H. G. Bohlen, and F. Nuoffer, *Nucl. Phys.* **A672**, 387 (2000).
  - [11] A. A. Ogloblin *et al.*, *Phys. At. Nucl.* **66**, 1478 (2003).
  - [12] S. Ohkubo and Y. Hirabayashi, *Phys. Rev. C* **70**, 041602(R) (2004).
  - [13] S. Ohkubo and Y. Hirabayashi, *Phys. Rev. C* **75**, 044609 (2007).
  - [14] Sh. Hamada, Y. Hirabayashi, N. Burtbayev, and S. Ohkubo, *Phys. Rev. C* **87**, 024311 (2013).
  - [15] S. Ohkubo and Y. Hirabayashi, *Phys. Rev. C* **89**, 051601(R) (2014).
  - [16] S. Ohkubo and Y. Hirabayashi, *Phys. Rev. C* **89**, 061601(R) (2014).
  - [17] S. Ohkubo, Y. Hirabayashi, A. A. Ogloblin, Yu. A. Glukhov, A. S. Dem'yanova, and W. H. Trzaska, *Phys. Rev. C* **90**, 064617 (2014).
  - [18] R. S. Mackintosh, Y. Hirabayashi, and S. Ohkubo, *Phys. Rev. C* **91**, 024616 (2015).
  - [19] S. Ohkubo and Y. Hirabayashi, *Phys. Rev. C* **92**, 024624 (2015).
  - [20] Yu. A. Glukhov, V. P. Rudakov, K.P.Artemov, A. S. Dem'yanova, A. A. Ogloblin, S. A. Goncharov, and A. Izadpanakh, *Phys. At. Nucl.* **70**, 1 (2007).
  - [21] F. Michel, S. Ohkubo, and G. Reidemeister, *Prog. Theor. Phys. Suppl.* **132**, 7 (1998) and references therein.
  - [22] S. Ohkubo, T. Yamaya, and P. E. Hodgson, *Nuclear clusters. in Nucleon-Hadron Many-Body Systems*, (edited by H. Ejiri and H. Toki) (Oxford University Press, Oxford, UK, 1999), p. 150.
  - [23] S. Ohkubo and K. Yamashita, *Phys. Lett.* **B578**, 304 (2004).
  - [24] S. Ohkubo and Y. Hirabayashi, *Phys. Lett.* **B684**, 127 (2010).
  - [25] Y. Hirabayashi and S. Ohkubo, *Phys. Rev. C* **88**, 014314 (2013).
  - [26] K. W. Ford and J. A. Wheeler, *Ann. Phys. (N. Y.)* **7**, 259 (1959).
  - [27] R. G. Newton, *Scattering Theory of Waves and Particles* (McGraw-Hill Book Company, New York, 1966).
  - [28] P. E. Hodgson, *Nuclear Heavy-Ion Reactions* (Oxford Studies in Nuclear Physics, Clarendon Press: Oxford University Press, Oxford, UK, 1978).
  - [29] D. M. Brink, *Semi-classical Methods for Nucleus-Nucleus Scattering* (Cambridge University Press, Cambridge, 1985).
  - [30] A. S. Dem'yanova *et al.*, in *AIP Conference Proceedings on International Symposium on Exotic Nuclei*, edited by Yu. E. Penionzhkevich and S. M. Lukyanov, **1224**, 82 (2010); A. S. Dem'yanova *et al.*, *Nucl. Phys.* **A834**, 473c (2010).
  - [31] H. De Vries, C. W. De Jager, and C. De Vries, *At. Data and Nucl. Data Tables* **36**, 495 (1987); J. Heisenberg, J. S. McCarthy, and I. Sick, *Nucl. Phys.* **157**, 435 (1970).
  - [32] M. Kamimura, *Nucl. Phys.* **A351**, 456 (1981).
  - [33] W. J. Vermeer, M. T. Esat, J. A. Kuehner, R. H. Spear, A. M. Baxter, and S. Hinds, *Phys. Lett.* **122B**, 23 (1983).
  - [34] A. M. Kobos, B. A. Brown, P. E. Hodgson, G. R. Satchler, and A. Budzanowski, *Nucl. Phys.* **A384**, 65 (1982); A. M. Kobos, B. A. Brown, R. Lindsay, and G. R. Satchler, *Nucl. Phys.* **A425**, 205 (1984). G. Bertsch, J. Borysowicz, H. McManus, and W. G. Love, *Nucl. Phys.* **A284**, 399 (1977).
  - [35] D. T. Khoa, W. von Oertzen, and H. G. Bohlen, *Phys. Rev. C* **49**, 1652 (1994).
  - [36] G. R. Satchler and W. G. Love, *Phys. Rep.* **55**, 183 (1979).
  - [37] M. E. Brandan and G. R. Satchler, *Phys. Rep.* **285**, 143 (1997).
  - [38] D. T. Khoa, *Phys. Rev. C* **63**, 034007 (2001).
  - [39] G. R. Satchler, *Direct Nuclear Reactions* (Oxford University Press, Oxford, 1983).
  - [40] H. G. Bohlen, X. S. Chen, J. G. Cramer, P. Fröbich, B. Gebauer, H. Lettau, A. Miczaika, W. von Oertzen, R. Ulrich, and T. Wilpert, *Z. Phys. A* **322**, 241 (1985).
  - [41] A. S. Dem'yanova *et al.*, *IAEA Database exfor*, <http://www.nds.iaea.org/exfor/>.